

A Quantum Computation Model for Molecular Nanomagnets

Original

A Quantum Computation Model for Molecular Nanomagnets / Cirillo, Giovanni Amedeo; Turvani, Giovanna; Graziano, Mariagrazia. - In: IEEE TRANSACTIONS ON NANOTECHNOLOGY. - ISSN 1536-125X. - 18:(2019), pp. 1027-1039. [10.1109/TNANO.2019.2939910]

Availability:

This version is available at: 11583/2761452 since: 2019-12-05T12:10:15Z

Publisher:

IEEE

Published

DOI:10.1109/TNANO.2019.2939910

Terms of use:

openAccess

This article is made available under terms and conditions as specified in the corresponding bibliographic description in the repository

Publisher copyright

(Article begins on next page)

A quantum computation model for molecular nanomagnets

Giovanni Amedeo Cirillo, *Student Member, IEEE*, Giovanna Turvani, and Mariagrazia Graziano, *Member, IEEE*

Abstract—Molecular nanomagnets can be considered as serious candidates for the definition of a scalable and reliable quantum computing technology: information is encoded on their spins and they ensure relaxation and decoherence times sufficiently long for the execution of tens of quantum operations. Among these devices, Cr_7Ni supramolecular complexes are extremely of interest since they implement a universal set of quantum gates, made of single-qubit gates and the two-qubit Controlled-phase gate. A model for analyzing Cr_7Ni molecules and a potential quantum computer architecture are proposed: starting from the energy parameters required for spin manipulations, these systems have been proved to implement elementary quantum algorithms. Within this paper, two, three and four-qubit systems have been analyzed: the simulation of quantum operations and the analysis of dynamical non-idealities have been done in parallel. Our approach enables the definition of an operating point - in terms of magnetic driving fields and latency - in which the execution of elementary quantum algorithms is characterized by negligible errors. The proposed model has been entirely implemented in MATLAB, thus obtaining a software infrastructure for the analysis of Cr_7Ni molecules that can be extended to quantum systems with analogous Hamiltonian and behavior.

Index Terms—Molecular Nanomagnets, Quantum Computing Architectures, Quantum Algorithms, Innovative Technology

I. INTRODUCTION

The high-power consumption due to leakage currents and the technological limits of lithography-based techniques used for fabrication are making the development of Complementary Metal-Oxide-Semiconductor (CMOS) technology increasingly harder, with the consequent risk that the computation performance scaling in the next decades cannot be ensured. In order to overcome these limitations, two different approaches have been considered: on the one hand, research can focus on technologies which can inherit the CMOS role of leading technology for the production of microprocessors based on deterministic binary information and boolean logic [1] (the so-called **classical computers**); on the other, new computing paradigms - alternative to the classical one - can be analyzed. **Quantum Computation** belongs to this set: its unit of information, named **qubit**, is physically mapped on a quantum state (e.g. a spin) instead of a classical state as a voltage. Since quantum states are characterized by superposition, the qubit has a non-null probability of being in two different

states (encoding 0 and 1) at the same time [2]. Superposition permits to define an equivalent parallel computation model, involving quantum algorithms faster than the corresponding classical ones, in terms of computational costs. For example, a quantum computer is able to execute in polynomial time prime factoring, which requires exponential time in Boolean-based computation [3].

Many technologies have been proposed for implementing a quantum computer based on superconductivity [4]–[7], trapped ions [8], photons [9], [10], technologies (ultracold atoms in optical lattices, thin-film superconductors, Semiconductor Heterostructures) for topological quantum computing [11], [12] and spin systems as quantum-dots [13], silicon [14]–[16] and molecules [17]–[21], which can be as organic as inorganic [22]. Molecular quantum information is encoded on spin orientations and qubits are manipulated through magnetic resonance techniques. Many quantum algorithms have been executed on apparatus for liquid-state NMR spectroscopy [23]–[30]. The molecules typically employed for NMR quantum information processing usually encode information on nuclear spins of hydrogen, carbon and fluorine atoms. The main limitation of this technology is related to the scaling of the number of qubits, through the synthesis of more complex molecules with more spin qubits; for this reason, the analysis of alternative molecular technologies for quantum computing would permit to overcome these limitations. Among spin-qubit technologies, we focused our attention on molecular nanomagnets, that result extremely interesting not only for the capability of scaling the number of qubits through supramolecular chemistry techniques, but also for their long relaxation and decoherence timescales, enabling the implementation of tens of quantum operations with negligible errors. In particular with this work, $\text{Cr}_7\text{Ni-Co-Cr}_7\text{Ni}$ molecular nanomagnets, which has been proved to implement a universal set of quantum gates [31] - have been analyzed. Starting from these properties, we present here a simulation and validation model, entirely developed in MATLAB, for the analysis of the execution of quantum operations and algorithms with these molecules. This *bottom-up* methodology can be further exploited for the investigation of other molecular technologies that can be candidates for the definition of a future quantum computer architecture. After an overview of quantum computation fundamentals and the state of the art for quantum computing with molecular nanomagnets, the Cr_7Ni -qubit model is presented, focusing on the universal set of quantum gates of this technology. In Section V a potential quantum computer architecture is proposed, with the Cr_7Ni complex behaving as a processing unit. An overview of the implemented instructions, exploitable for simulating

The authors are with the Electronics and Telecommunications Department of Politecnico di Torino, Torino, 10129, Italy (e-mail: giovanni_cirillo@polito.it; giovanna.turvani@polito.it; mariagrazia.graziano@polito.it).

Copyright (c) 2019 IEEE. Personal use of this material is permitted. However, permission to use this material for any other other purposes must be obtained from the IEEE by sending a request to pubs-permissions@ieee.org.

elementary quantum algorithms up to four qubits, is reported. In Section VI non-idealities are analyzed, in order to define a quasi-optimal operating point for the molecular processor. In Section VIII the results obtained from the simulation of a three-qubit algorithm are reported. Future perspectives for the technology and modeling infrastructure are reported in Section IX.

II. BACKGROUND

The quantum unit of information is the qubit; it is encoded on a quantum physical system with two basis states - typically named $|0\rangle$ and $|1\rangle$ - implemented in many ways, as spin states of electrons, atomic energy levels, polarization states of photons, or paths in an interferometer. In quantum circuit and information theories the qubit is abstracted from physical details. The main difference between a qubit and a classical bit is that the first is not confined to one of the states $|0\rangle$ and $|1\rangle$, but can be found in arbitrary **superposition** states

$$|\psi\rangle = c_0 |0\rangle + c_1 |1\rangle = c_0 \cdot \begin{bmatrix} 1 \\ 0 \end{bmatrix} + c_1 \cdot \begin{bmatrix} 0 \\ 1 \end{bmatrix} = \begin{bmatrix} c_0 \\ c_1 \end{bmatrix} \quad (1)$$

where $c_0, c_1 \in \mathbb{C}$ are the probability amplitudes, each one associated to one qubit basis state. The square magnitude of each probability amplitude is equal to the probability of finding the qubit in the corresponding state, thus $|c_0|^2 = P(|\psi\rangle = |0\rangle)$, $|c_1|^2 = P(|\psi\rangle = |1\rangle)$ and $|c_0|^2 + |c_1|^2 = 1$. For these reasons, the qubit can be in two different states (encoding 0 and 1) at the same time. The one-qubit model can be generalized to a **quantum register** of N qubits with 2^N basis states $|\psi\rangle = \sum_{i=0}^{2^N-1} c_i |\psi_i\rangle$, with $|c_i|^2 = P(|\psi\rangle = |\psi_i\rangle)$ and $\sum_{i=0}^{2^N-1} |c_i|^2 = 1$. Superposition is the property permitting to quantum bits of being more powerful than their classical equivalents, since a higher degree of computing parallelism can be exploited by employing qubits, given the same number N of information units. However, qubit's superposition is suppressed when the qubit value is measured; for this reason, measurement must be executed only at the end of the sequence of operations required by a certain quantum algorithm.

Any state of the qubit can be represented as a unit vector in the Cartesian space connecting the origin and a point on the surface of the Bloch sphere (Figure 1). The state vector

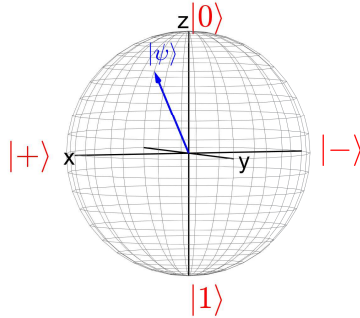


Figure 1. Bloch sphere in the Cartesian space. The north and south poles correspond to basis states $|0\rangle$ and $|1\rangle$, while $|\pm\rangle = \frac{|0\rangle \pm |1\rangle}{\sqrt{2}}$.

can be written as $|\psi\rangle = \cos\left(\frac{\theta}{2}\right) |0\rangle + e^{i\phi} \sin\left(\frac{\theta}{2}\right) |1\rangle$, where $0 \leq \theta \leq \pi$ is the co-latitude angle and $0 \leq \phi \leq 2\pi$ is

the azimuth angle. The two basis states $|0\rangle$ ($\theta = 0$) and $|1\rangle$ ($\theta = \pi$) - corresponding to the states 0 and 1 of a classical bit - lie at the poles of the sphere; in these cases the value of ϕ is irrelevant. **Points on the same latitude have the same probabilities** $|c_0|^2$ and $|c_1|^2$.

Operations on a qubit correspond to moving the state vector, thus eventually changing its probabilities of being $|0\rangle$ or $|1\rangle$, through **rotations of the Cartesian axes** described by matrices $R_x(\theta)$, $R_y(\theta)$, $R_z(\theta)$ [2]. They are related to the well-known **Pauli matrices** σ_x , σ_y and σ_z - typically employed for the description of two-level quantum systems - by the following equations:

$$R_{x,y,z}(\theta) = e^{-i\frac{\theta}{2}\sigma_{x,y,z}} = \cos\left(\frac{\theta}{2}\right) I + i \sin\left(\frac{\theta}{2}\right) \sigma_{x,y,z},$$

$$(\sigma_{x,y,z})^{\frac{\theta}{\pi}} = e^{i\frac{\theta}{2}} R_{x,y,z}(\theta), \quad (2)$$

where I is the identity matrix. For example, $(\sigma_x)^{\frac{1}{2}} = e^{i\frac{\pi}{4}} R_x\left(\frac{\pi}{2}\right)$ and $\sigma_z = e^{i\frac{\pi}{2}} R_z(\pi)$. It must be observed that quantum gates implemented by real quantum computers are typically characterized by phase shifts of type $e^{i\phi}$ that do not affect the final result. In fact, if a generic quantum gate $e^{i\phi}M$ is applied on the quantum state $|\psi\rangle$, resulting in a final state $|\psi'\rangle = e^{i\phi}M|\psi\rangle = e^{i\phi}|\psi_M\rangle$, the scalar term does not affect any probability $|\langle\psi'_j|\psi'\rangle|^2$ of the final state since $|\langle\psi'_j|\psi'\rangle|^2 = |e^{i\phi}|^2 \cdot |\langle\psi_M|\psi_M\rangle|^2 = |\langle\psi_M|\psi_M\rangle|^2$.

According to the vector description of qubit, any quantum gate involving k qubits can be described by a $2^k \times 2^k$ unitary matrix which modifies the probability amplitudes of a state vector of length 2^k .

III. QUANTUM COMPUTING WITH MOLECULAR NANOMAGNETS

Single-Molecule Magnets (SMMs) are coordination compounds that show magnetic bistability and an energy barrier for magnetization reversal. Moreover, they display slow relaxation of the magnetization at the single-molecule level (not involving any intermolecular interaction), so when the molecule is magnetized in presence of a magnetic field, it will retain its magnetization on removal of the field. They are based on a core of magnetic ions surrounded by ligands eventually exploited for linking different spin systems, thus allowing the implementation of scalable multi-qubit devices.

For the energy analysis of these systems, a static field $\mathbf{B} = B\mathbf{z}$ is supposed to be applied on the molecule and their characteristic spin magnetic moment tends to align with the axis of the static field, with an orientation that minimizes energy. If an energy amount is provided to the system, the spin orientation changes, so it can be exploited for encoding information; moreover, since spin is a typical quantum mechanics quantity, quantum information can be encoded. It is possible to consider two different spin quantum numbers: the primary S - that is constant - and the secondary S_z , related to the projection of the molecule's magnetic moment along the z -axis and depending on the spin energy, ranging from $-S$ to $+S$ in steps of one, so the total number of states is $2S + 1$.

Molecular nanomagnets - as any candidate technology for

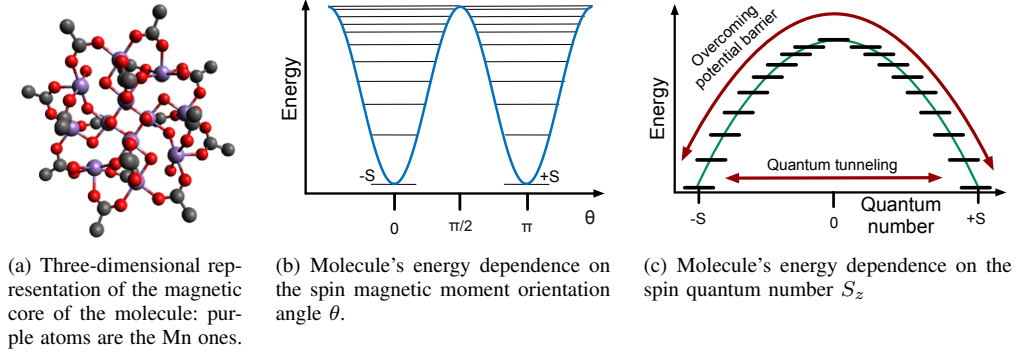


Figure 2. Mn_{12} Single Molecule Magnet: molecular core of the magnet and energy characteristics. The two plots refer to the same energy depending on two different variables, so the heights of the potential barriers are exactly the same. Energy dependencies on the orientation angle θ and S_z present the same shapes for the Fe_8 SMM.

quantum computing - must ensure the implementability of an universal set of quantum gates, an efficient addressability of qubits (*i.e.* the application of an excitation on a certain qubit must not influence the others) and long coherence timescales. Theoretical chemistry provides an important role in their engineering, in particular for what concerns the modelling of spin dynamics, which has a fundamental role in the definition of design methodologies for molecular nanomagnets with long relaxation and coherence timescales. In order to have more accurate models describing the non-idealities of spin qubits, efforts on integrating the spin-phonon interaction - which is recognized as a critical parameter for having slow relaxation of magnetization - into the computational methodologies of spin relaxation - mainly based on the analysis of the SMM energy barrier - are currently made [32].

From an historical point of view, Fe_8 and Mn_{12} have been the most studied molecular nanomagnets. For these molecules, $S = 10$ and the spin magnetic moment minimizes its energy when it is oriented parallel or anti-parallel to the static field ($\theta \in \{0, \pi\}$). Information can be encoded:

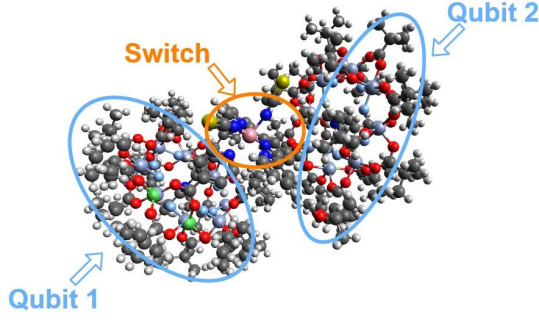
- on the energy states with $S_z = \pm S$, *i.e.* $|0\rangle$ and $|1\rangle$ are defined on anti-parallel orientations. Spin can be changed by providing an energy amount either for overcoming the parabolic potential barrier in Figure 2 or sufficient for quantum tunneling, thus permitting the direct magnetization reversal from $-S$ to $+S$ (and *vice versa*);
- on two adjacent energy states (*e.g.* $|0\rangle \leftrightarrow S_z = -S$ and $|1\rangle \leftrightarrow S_z = -S + 1$);
- on more than two states, since a molecular magnet with $N = 2S + 1$ states can be exploited to encode $\lceil \log_2(N) \rceil$ bits.

In 2001 it was proved that Fe_8 and Mn_{12} single molecule magnets are candidates for the realization of a quantum computer - according to the DiVincenzo's criteria [33] - capable to solve Grover's algorithm [34]. More recently, other molecular technologies based on transition metal complexes [35] or lanthanides [36] have been proposed for spin quantum computing [37]. Some of them are based on multi-level systems as GdW_{30} single-ion magnet [38], [39], where the Gd^{3+} ion presents $S = \frac{7}{2}$, and the TbPc_2 SMM, where quantum information is encoded on the electrically-drivable

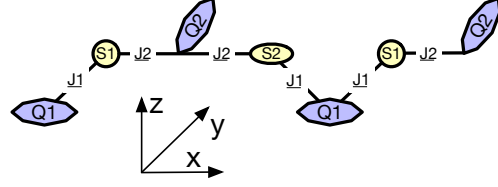
nuclear spin- $\frac{3}{2}$ of the Tb^{3+} ion. The second molecule can be embedded in a Single-Electron Transistor and it has been experimentally proved to implement the iSWAP two-qubit gate [40] and the Grover's search algorithm [41]. These multi-level devices present many difficulties for the implementation of a universal set of quantum gates with independent and addressable qubits, which is one of the main goals of quantum technology research. Moreover, the main problem of molecular magnets with $S > \frac{1}{2}$ is their modest decoherence timescale, with the consequent limitation to the maximum number of operations executable with negligible error. In fact, it has been experimentally proved [42] that T_2 values for molecules with $S = \frac{1}{2}$ are some order of magnitude longer than those for $S > \frac{1}{2}$, typically in the order of magnitude of $1\mu\text{s}$ - $10\mu\text{s}$. The currently longest coherence timescale for a molecular nanomagnet $T_2 \approx 0.7\text{ms}$ belongs to the spin- $\frac{1}{2}$ of a vanadium(IV) trisdithiolate platform ($[\text{V}(\text{C}_8\text{S}_8)_3]^{2-}$) diluted in nuclear spin-free solvent CS_2 at cryogenic temperatures [43]. If a molecule presents more spins, they can be exploited as independent qubits. This is the case of the dinuclear complex of terbium or dysprosium ions [44], [45] and Cr_7Ni supramolecular complexes [31]: the first ones exploit the misalignment of the easy axes and the different gyromagnetic ratios of two spins to obtain a four-level quantum system implementing CNOT and SWAP quantum gates, but their scalability seems to be difficultly provable, while the others do not only present high decoherence timescales (reach $T_2 \sim 15\mu\text{s}$ [46]) compared with the other molecular nanomagnets for quantum computing and the capability of implementing a universal set of quantum gates, but they are also scalable. A detailed analysis of these devices is available in the following sections.

IV. Cr_7Ni SUPRAMOLECULAR COMPLEXES

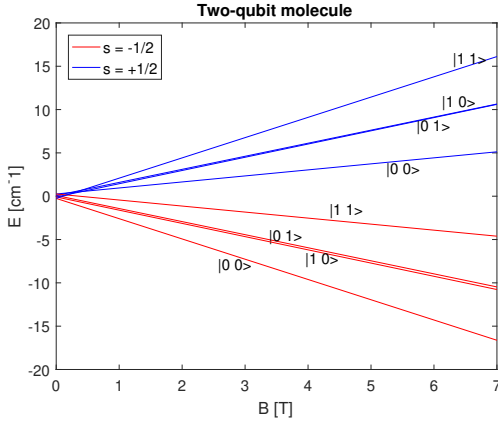
Each Cr_7Ni ring presents a characteristic spin with $S = \frac{1}{2}$ that is exploited for the definition of a qubit. Assemblies of low-spin coupling rings have been made through switchable links, that are also characterized by a spin- $\frac{1}{2}$ at low temperature ($T = 5\text{K}$). Supramolecular chemistry is exploited to link individual components with different spatial configurations, thus influencing the properties of the resulting supramolecules. When the switch between two qubits is frozen in its ground



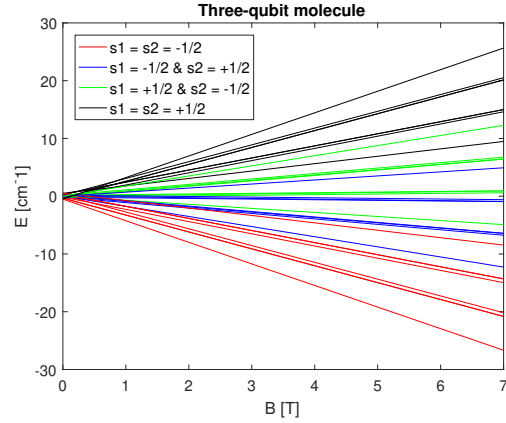
(a) Two-qubit molecule with two Cr_7Ni rings (see light blue atoms) [31], each one encoding one qubit, and the intermediate Co^{2+} ion (pink atom in the middle), associated to the spin switch.



(b) Conceptual scheme of a four-qubit complex, where **Q** and **S** refer to a spin qubit and a spin switch respectively: the periodical structure and the different easy axes of spin qubits connected to the same switch are highlighted.



(c) Zeeman diagram of a two-qubit molecule [47] (three spins).



(d) Zeeman diagram of a three-qubit molecule [47] (five spins)

Figure 3. Cr_7Ni supramolecular complexes and energy levels for two and three-qubit molecules: s refers to the switch spin secondary quantum number S_z , thus its orientation. Each energy level is associated to a possible combination of the spins orientations; in particular, the red curves are those where each spin switch presents "open" orientation.

state ($|S_z\rangle = |-\frac{1}{2}\rangle$), they can be treated as decoupled on a timescale of 500 ns when a magnetostatic field $B \sim 5$ T is applied, so single qubit gates $R_x(\theta)$, $R_y(\theta)$ and $R_z(\theta)$ can be implemented by magnetic pulses resonant with the qubit gap. On the other hand, conditional gates between neighboring pairs of qubits are performed by temporarily bringing the switch spin to an excited state, where it changes its orientation ($|S_{z_{sw}}\rangle = |+\frac{1}{2}\rangle$) [31], [47]. The spin- $\frac{1}{2}$ unitary matrix, describing the evolution of qubits and switches, is available in Appendix A.

A couple of Cr_7Ni rings is connected through high spin Co^{2+} ions. From the analysis of two and three-qubit molecules [31], [47], it is possible to write a general $2N - 1$ spin- $\frac{1}{2}$ Hamiltonian operator for N qubits and $N - 1$ switches, according to the schematic representation - to be read from left to right - of the supramolecular complex in Figure 3(b):

$$\begin{aligned} \frac{\hat{H}}{\hbar} = & \mu_B \sum_{i=1}^N (\mathbf{Q}_i \cdot \mathbf{g}_{i_{\text{qubit}}} \cdot \mathbf{B}) + \mu_B \sum_{i=1}^{N-1} (\mathbf{S}_i \cdot \mathbf{g}_{i_{\text{sw}}} \cdot \mathbf{B}) \\ & + \sum_{i=1}^{N-1} (\mathbf{Q}_i \cdot \mathbf{J}_{i_{\text{qubit}}, i_{\text{sw}}} \cdot \mathbf{S}_i) + \sum_{i=1}^{N-1} (\mathbf{S}_i \cdot \mathbf{J}_{i_{\text{sw}}, i+1_{\text{qubit}}} \cdot \mathbf{Q}_{i+1}), \end{aligned} \quad (3)$$

where \mathbf{Q}_i and \mathbf{S}_i are effective spin- $\frac{1}{2}$ operators vectors (e.g. $\mathbf{Q} = \mathbf{Q}_x \hat{x} + \mathbf{Q}_y \hat{y} + \mathbf{Q}_z \hat{z} = \frac{1}{2} \sigma_x \hat{x} + \frac{1}{2} \sigma_y \hat{y} + \frac{1}{2} \sigma_z \hat{z} =$

$\frac{1}{2} \vec{\sigma}$) of the i^{th} Cr_7Ni and the i^{th} Co^{2+} spins respectively, $\underline{J} = \text{diag}([J_x, J_y, J_z])$ is the anisotropic exchange tensor describing the interaction between adjacent spins, $\underline{g} = \text{diag}([g_x, g_y, g_z])$ is the spectroscopic tensor describing the interaction of the magnetic moments with an external magnetic field \mathbf{B} and μ_B is the Bohr magneton. Considering Figure 3(b), the molecule presents a periodical structure, where all the operators assume only two values in a regular way: $\mathbf{Q}_i = \mathbf{Q}_{1(2)}$, $\mathbf{S}_i = \mathbf{S}_{1(2)}$, $\underline{J}_{i_{\text{qubit}}, i_{\text{sw}}} = \underline{J}_{1(2)}$ and $\underline{J}_{i_{\text{sw}}, i+1_{\text{qubit}}} = \underline{J}_{2(1)}$ when i is odd(even). Moreover, spin qubits "linked" to the same spin switch have perpendicular easy axes due to different \underline{J} and \underline{g} interactions. The parameters of the molecule employed in simulations are available in [31] and [47].

The Zeeman diagram for a static field along the z -axis - with the energy levels of the two and three-qubit molecules - are available in Figures 3(c) and 3(d): energies are reported in terms of wavelength reciprocal (cm^{-1}), so the equivalence $f [\text{GHz}] \simeq 30 \cdot \lambda^{-1} [\text{cm}^{-1}]$ can be exploited for interpreting them in terms of frequency. For the analysis of these devices, it must assumed that **qubits and switches are never entangled**, so a quantum system made of N qubits and $N - 1$ switches can be described by two independent state vectors with 2^N

and 2^{N-1} probability amplitudes respectively:

$$|\psi\rangle_{\text{system}} = |\psi\rangle_{\text{qubits}} \otimes \left(|S_{z_{\text{sw}}}\rangle = \left| -\frac{1}{2} \right\rangle \right)^{\otimes N-1}, \quad (4)$$

where \otimes refers to the tensor product. The **computational basis** is defined for states where the spin of each switch is $|S_{z_{\text{sw}}}\rangle = \left| -\frac{1}{2} \right\rangle$ (red curves), *i.e.* the spin switch is in its ground state. For each qubit, $|0\rangle$ and $|1\rangle$ are encoded on qubit spin states $|S_{z_{\text{qubit}}}\rangle = \left| -\frac{1}{2} \right\rangle$ and $|S_{z_{\text{qubit}}}\rangle = \left| +\frac{1}{2} \right\rangle$ respectively. The "open switch" states are exploited for the implementation of single-qubit gates: magnetic anisotropy is responsible of the different transition frequencies of spin qubits (*e.g.* $\Delta f_{|00\rangle \rightarrow |01\rangle} \neq \Delta f_{|00\rangle \rightarrow |10\rangle}$), thus allowing to independently rotate them. The total transition energy/frequency from ground state $|000\rangle$ to a state with two or more qubits equal to $|1\rangle$ is the sum of those of each separate spin, *e.g.* the rotation energy required for the $|000\rangle \rightarrow |101\rangle$ transition would be $\Delta E_{101} = \hbar(\omega_{001} + \omega_{100})$. For a magnetostatic field $B \leq 7$ T, the single-qubit transition frequencies all belong to the microwave spectrum.

Magnetic anisotropy is also responsible of a **transition frequency shift of the spin switch** depending exclusively on the states of the adjacent spin qubits. For a two-qubit molecule

$$\begin{aligned} \Delta f_{|00\rangle \otimes (|S_{z_{\text{sw}}}\rangle = \left| -\frac{1}{2} \right\rangle) \rightarrow |00\rangle \otimes (|S_{z_{\text{sw}}}\rangle = \left| +\frac{1}{2} \right\rangle)} &\neq \\ \Delta f_{|01\rangle \otimes (|S_{z_{\text{sw}}}\rangle = \left| -\frac{1}{2} \right\rangle) \rightarrow |01\rangle \otimes (|S_{z_{\text{sw}}}\rangle = \left| +\frac{1}{2} \right\rangle)} &\neq \\ \Delta f_{|10\rangle \otimes (|S_{z_{\text{sw}}}\rangle = \left| -\frac{1}{2} \right\rangle) \rightarrow |10\rangle \otimes (|S_{z_{\text{sw}}}\rangle = \left| +\frac{1}{2} \right\rangle)} &\neq \\ \Delta f_{|11\rangle \otimes (|S_{z_{\text{sw}}}\rangle = \left| -\frac{1}{2} \right\rangle) \rightarrow |11\rangle \otimes (|S_{z_{\text{sw}}}\rangle = \left| +\frac{1}{2} \right\rangle)} &\neq \end{aligned} \quad (5)$$

For a molecule with more than two qubits, it has been proved that spin switch transition frequency is only affected by its adjacent spin qubits and not by the others. This phenomenon is exploited for the implementation of the two-qubit Controlled-phase ($C\phi$) gate

$$C\phi = \begin{bmatrix} 1 & 0 & 0 & 0 \\ 0 & 1 & 0 & 0 \\ 0 & 0 & 1 & 0 \\ 0 & 0 & 0 & e^{i\phi} \end{bmatrix}. \quad (6)$$

In order to easily derive the unitary evolution matrix of the $C\phi$ gate in these molecules, it is convenient to analyze the evolution of each basis state ($|00\rangle, \dots, |11\rangle$) separately. In fact, each column of the unitary matrix corresponds to the evolution of one basis vector; for a 4×4 matrix, the leftmost column refers to the evolution of $|00\rangle = [1, 0, 0, 0]^T$, while the rightmost refers to $|11\rangle = [0, 0, 0, 1]^T$. In these devices, the $C\phi$ gate is realized by a couple of oscillating π -pulses resonant with the transition $|11\rangle \otimes (|S_{z_{\text{sw}}}\rangle = \left| -\frac{1}{2} \right\rangle) \Leftrightarrow |11\rangle \otimes (|S_{z_{\text{sw}}}\rangle = \left| +\frac{1}{2} \right\rangle)$. When the spin qubits are both $|1\rangle$, the spin switch is rotated and it accumulates two phases contributions (see Appendix A for the computation of their values), one per rotation, thus obtaining a total phase shift $e^{i\phi}$ depending on the

difference of the phases of the two consecutive oscillations:

$$\begin{aligned} |11\rangle \otimes \left(|S_{z_{\text{sw}}}\rangle = \left| -\frac{1}{2} \right\rangle \right) &\xrightarrow[f = \Delta f_{|11\rangle}, \phi = -\phi_1]{\text{First } \pi \text{ pulse}} |11\rangle \otimes \left[|S_{z_{\text{sw}}}\rangle = e^{-i(\frac{\pi}{2} + \phi_1)} \left| +\frac{1}{2} \right\rangle \right] \\ &\xrightarrow[f = \Delta f_{|11\rangle}, \phi = \pi - \phi_2]{\text{Second } \pi \text{ pulse}} |11\rangle \otimes \left[|S_{z_{\text{sw}}}\rangle = e^{i(\phi_2 - \phi_1)} \left| -\frac{1}{2} \right\rangle \right]. \end{aligned} \quad (7)$$

Then, according to the tensor product property $A \otimes kB = kA \otimes B$, where A and B are two vectors and k a scalar term, it is possible to "pass" the accumulated phase contribution to the qubit state vector

$$\begin{aligned} |11\rangle \otimes \left(|S_{z_{\text{sw}}}\rangle = e^{i(\phi_2 - \phi_1)} \left| -\frac{1}{2} \right\rangle \right) &= \\ e^{i(\phi_2 - \phi_1)} |11\rangle \otimes \left(|S_{z_{\text{sw}}}\rangle = \left| -\frac{1}{2} \right\rangle \right) \end{aligned} \quad (8)$$

If qubits are not both equal to $|1\rangle$, the spin switch is not rotated (see inequalities in 6), so the evolution in Equation 7 does not take place and no phase amount to be provided to the qubit vector is accumulated. In conclusion, the global unitary evolution on the qubit state vector is the same of a $C\phi$ gate. According to [31], a couple of pulses - with carrier frequency resonant with the transition $|11\rangle \otimes (|S_{z_{\text{sw}}}\rangle = \left| -\frac{1}{2} \right\rangle) \Leftrightarrow |11\rangle \otimes (|S_{z_{\text{sw}}}\rangle = \left| +\frac{1}{2} \right\rangle)$ and modulated by a Gaussian function with peak value of 50 G and 99% of area in about 6 ns - permits to obtain the evolution of a CZ gate, *i.e.* a $C\phi$ with $\phi = \pi$.

The quantum gates of $\text{Cr}_7\text{Ni-Co-Cr}_7\text{Ni}$ supramolecular complexes have already been proved to be employable for **quantum simulation** [48]–[50]; in fact, since these are particular unitary evolutions of the spins qubits, they can be engineered such that the spin system of the molecular nanomagnet can mimic the dynamics of another quantum system. In particular, a three-qubit molecule can simulate the transverse field Ising model [47].

V. ARCHITECTURE

The previous results have been employed for developing a MATLAB model for the $\text{Cr}_7\text{Ni-Co-Cr}_7\text{Ni}$ supramolecular complexes, which has been thought for investigating the quantum algorithms that can be executed on the current molecules with negligible errors. The model has been constructed from **a theoretical description of a potential quantum computer architecture**, where the molecular nanomagnet can be treated as a Execution Unit. Computation is organized according to the so-called **quantum circuit model** [2], where all the operations are implemented as sequences of quantum gates which can be obtained in their turn by sequences of quantum gates belonging to a universal set. This model permits to interpret the architecture in a sort of microprogramming paradigm, where quantum gates belonging to a universal set behave as microinstructions exploitable for building a more complex instruction/quantum gate set. For this reason, the most effective approach for developing a sophisticated quantum computation model is starting from the elementary gates: the mathematical models for single-qubit and Controlled-phase gates are explained in

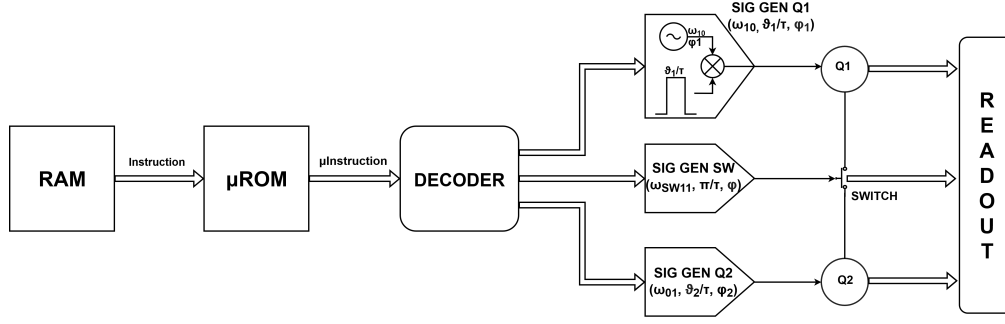


Figure 4. Conceptual block scheme of the proposed quantum computer architecture. Signal generators for manipulating the spin switch and qubit Q2 are equivalent to that for qubit Q1.

Appendices A, B.

The idea of the proposed architecture is mapping quantum computation onto spin manipulations and a **conceptual block scheme** of a two-qubit computer is presented in Figure 4; it is reiterated that the description is only theoretical and there is not any corresponding real hardware. It is possible to distinguish four parts:

- a memory system based on one classical Random-Access-Memory and one classical micro-Read-Only-Memory, where instructions/quantum gates to be executed are stored and translated into sequences of those of the universal set respectively;
- a front-end circuitry, for decoding each microinstruction into a sequence of spin manipulations;
- a molecular quantum Execution Unit;
- a back-end circuitry for the readout, that is only enabled at the end of the quantum program, in order to ensure qubit superposition during the whole execution.

It can be observed the only quantum part of the architecture is the molecule and the others are related on how spin qubits must be sequentially manipulated or measured. Error correction techniques have not been analyzed, thus implying that the qubits' non-idealities will inexorably affect the final results.

Spins are manipulated through Magnetic Resonance: an oscillating pulse of specific amplitude, frequency and phase is applied on spin qubits for single-qubit gates or on the Co switch for implementing the $C\phi$ gate. Critical parameters for manipulating spins are the phase of the carrier and spin's rotation amount θ , that is equal - according to the Magnetic Resonance theory - to the product between the precession frequency around the xy plane ω_1 - depending on the spin gyromagnetic ratio γ - and the time duration τ , supposing a modulating rectangular pulse. In the proposed theoretical architecture, oscillating magnetic fields are assumed to be generated by appropriate spin manipulation signal generators (SIG GEN in Figure 4), where τ is fixed and belonging to the [5; 10]ns range for a two-qubit molecule - as in the simulation available in [31] - and the amplitude and phase of oscillations are the variable parameters. The generated signals must reach the transition frequencies of the spins of interest - in this case in the microwave spectrum - and the frequency spectrum of the modulating signal must not have too intense harmonics

at the transition frequencies different from the chosen one, in order to avoid undesired spin rotations. The described architecture seems to be capable of totally satisfying in future the DiVincenzo criteria for the physical implementation of a quantum computer [51].

A. Microinstructions

$R_x(\theta)$, $R_y(\theta)$ and the $C\phi$ gates can be treated as the microinstructions of the proposed architecture. The two-single qubit gates differ for the phase of the oscillating pulse, that is equal to 0 and $\frac{\pi}{2}$ for rotations about x and y axes respectively. They constitute a **universal set of quantum gates**, which is proved to be **alternative and equivalent to the well-known Clifford+T set** - made of Hadamard, S , T and CNOT gates [2] - in the following. In fact, sequences of these gates implement the Clifford+T ones except for a negligible phase contribution (see the ending part of Section I).

The **Hadamard** gate works on single qubits with matrix

$$H = \frac{1}{\sqrt{2}} \begin{bmatrix} 1 & 1 \\ 1 & -1 \end{bmatrix}. \quad (9)$$

After applying this gate to $|0\rangle$ or $|1\rangle$, a measurement will have equal probabilities to become 0 or 1 ($|0\rangle \rightarrow \frac{|0\rangle+|1\rangle}{\sqrt{2}} = |+\rangle$ and $|1\rangle \rightarrow \frac{|0\rangle-|1\rangle}{\sqrt{2}} = |-\rangle$); for this reason, it is typically employed at the beginning of quantum algorithms, in order to obtain an equal superposition of states. A unitary evolution equivalent to the Hadamard gate can be obtained by

$$H = e^{i\frac{\pi}{2}} R_x(\pi) R_y\left(\frac{\pi}{2}\right). \quad (10)$$

The **S and T gates** are nothing but $R_z\left(\frac{\pi}{2}\right)$ and $R_z\left(\frac{\pi}{4}\right)$, except for a negligible scalar contribution $e^{i\frac{\theta}{2}}$. The implementation of these gates is ensured by the availability of $R_x(\theta)$ and a Hadamard-like gate. In fact, any rotation about the Cartesian z -axis can be obtained as

$$R_z(\theta) = H R_x(\theta) H. \quad (11)$$

Considering Equations 10 and 11, it is possible to prove that rotations about x and y axes are sufficient for obtaining any rotation about the z , with an additional scalar contribution

$e^{i(\pi + \frac{\theta}{2})}$. The two-qubit **Controlled-NOT** (CNOT) gate involves a control qubit and a target qubit. According to its unitary matrix

$$\text{CNOT} = \begin{bmatrix} 1 & 0 & 0 & 0 \\ 0 & 1 & 0 & 0 \\ 0 & 0 & 0 & 1 \\ 0 & 0 & 1 & 0 \end{bmatrix}, \quad (12)$$

the probability amplitudes of $|10\rangle$ and $|11\rangle$ are swapped, so the target qubit is flipped when the control is 1. This gate can be implemented on the device of interest by cascading a Hadamard gate on the target qubit, a CZ gate and another Hadamard gate on the target qubit (see the first equivalence in Figure 5).

B. Instruction set

From the considered universal set of quantum gates it has been possible to build a library of multi-qubit gates (Figures 5 and 6) to be simulated - with the parallel analysis of non-idealities reported in Sections VI and VII - on the $\text{Cr}_7\text{Ni-Co-Cr}_7\text{Ni}$ complexes.

The implemented quantum gates are reported in Figure 5: they involve non-adjacent qubits or they present swapped control and target qubits with the respect to standard gates [2]. Moreover, more complex multi-qubit gates on more complex molecules are obtainable (Figure 6), as the three-qubit **Toffoli** gate - with two control qubits and a target qubit which is toggled when the two controls are both 1 - and the reversible Half-Adder (through the **Peres gate**) and **Full-Adder** on three and four-qubit molecules respectively.

The library of quantum gates has also permitted the simulation on two, three and four-qubit molecules of algorithms as **Deutsch-Josza algorithm** [52], **Grover's algorithm** for searching an element in an unsorted array [53], [54], **Quantum Fourier Transform** (QFT), **Quantum Teleportation** for moving information from one qubit to another, **Entanglement Swapping** for entangling two non-adjacent qubits [55] and a **two-qubit adder** [56] (Figure 7).

VI. NON-IDEAL EFFECTS

In order to validate the architecture, it must be required that non-idealities do not affect significantly the system, thus not changing the results. Three dynamical effects must be taken into account:

- **spin relaxation**;
- **spin decoherence**;
- **residual inter-qubit interaction**, that does not ensure the complete insulation of the qubits when the switch is off.

These phenomena can be described by time constants, so a time duration on which they are negligible can be defined. It is recalled that spin relaxation is modeled by an exponential transient decay, where the probability of being in the higher energy state $|1\rangle$ is

$$P_{|1\rangle} = e^{-\frac{t}{T_1}}. \quad (13)$$

For the molecular magnet [31] $T_1 = 17.73(33)\mu\text{s}$, a value much greater than those associated to relaxation and qubit-qubit interaction, hence spin relaxation can be neglected.

A. Residual qubit-qubit interaction

When the Co switch is in the off state ($|S_{z_{sw}}\rangle = |-\frac{1}{2}\rangle$), it is not possible to consider the qubits isolated on an infinite timescale, *i.e.* a residual interaction depending on $\underline{J}_{1,2} \sim 1\text{ GHz}$ [31] is always present. Assuming that a static field B is applied on the z -axis and $g\mu_B B \gg \underline{J}_{1,2}$, the qubit-qubit interaction can be described by the following Hamiltonian, obtained by treating spin-spin interactions $\underline{J}_{1,2}$ as second-order perturbations of the Hamiltonian 3 for two qubits, with $|S_{z_{sw}}\rangle = |-\frac{1}{2}\rangle$ [47]:

$$\begin{aligned} \frac{\hat{H}_{\text{eff}}}{\hbar} = & \Gamma_{xx} \mathbf{Q}_{1x} \mathbf{Q}_{2x} + \Gamma_{yy} \mathbf{Q}_{1y} \mathbf{Q}_{2y} \\ & + \lambda_1 \mathbf{Q}_{1z} + \lambda_2 \mathbf{Q}_{2z} + C, \end{aligned} \quad (14)$$

where $\mathbf{Q}_{1k=\{x,y,z\}} = \mathbf{Q}_{k=\{x,y,z\}} \otimes I$ and $\mathbf{Q}_{2k=\{x,y,z\}} = I \otimes \mathbf{Q}_{k=\{x,y,z\}}$ are the spin operators of the two qubits. Apart from a constant term, Γ_{xx} and Γ_{yy} interactions (see [47] for the expressions) induce an unwanted evolution when the switch is turned off. The unwanted evolution can be controlled by the size of the applied field or by the size of the Co-ring exchange, in order to obtain high-fidelity single qubit gates. In the simulation of the Unwanted Evolution (UE), the effect of fast oscillations induced by the rotations of single spins around z (proportional to S_z) must be neglected, since they introduce a phase shift contribution which is not significant. It means that the unitary evolution of residual qubit-qubit interaction can be written as

$$U_{\text{UE}}(t) = e^{+\frac{i}{\hbar} \hat{H}_{\text{eff,diag}} \tau} e^{-\frac{i}{\hbar} \hat{H}_{\text{eff}} \tau}, \quad (15)$$

where $\hat{H}_{\text{eff,diag}}$ contains the terms on the main diagonal of the effective Hamiltonian. In order to estimate the effect of the unwanted evolution, the **fidelity**

$$\mathcal{F}(t) = \langle \psi_I(t) | \psi(t) \rangle, \quad (16)$$

is defined, where $|\psi_I(t)\rangle$ is the ideal evolution of the quantum state and $|\psi(t)\rangle = U_{\text{UE}}(t) |\psi(0)\rangle$ is the real evolution¹ due to inter-qubit interaction. In the absence of residual coupling no evolution occurs, so that $|\psi_I(t)\rangle = |\psi(0)\rangle$. The fidelity time evolutions of two two-qubit molecules - where the spin-spin interaction tensors \underline{J} are in one case those reported in [31] (blue curve), in the other one half of the previous ones (red curve) - for $B = 5\text{ T}$ are plotted in Figure 8(a). A reduction by a factor 2 of the Co-ring exchange is sufficient for increasing the timescale of the evolution, and consequently of the time durations with fidelity close to 1, by one order of magnitude. In order to establish a time duration in which the effect is negligible, the time intervals T_{UE} for which $\mathcal{F} \geq 0.9$ have been determined in function of the applied magnetic field. Moreover, since the right plot of Supplementary Figure 29 in [31] permits to estimate the dependency of T_{UE} in function of the number of qubits N as

$$T_{\text{UE}}(N) = T_{\text{UE}}(N-1) \cdot \frac{N-1}{N}, \quad (17)$$

the results in Figure 8(b) are reported for molecules characterized by a number of qubits from two to eight. Left and

¹It must be precised that for each non-ideal phenomenon, a different fidelity must be defined.

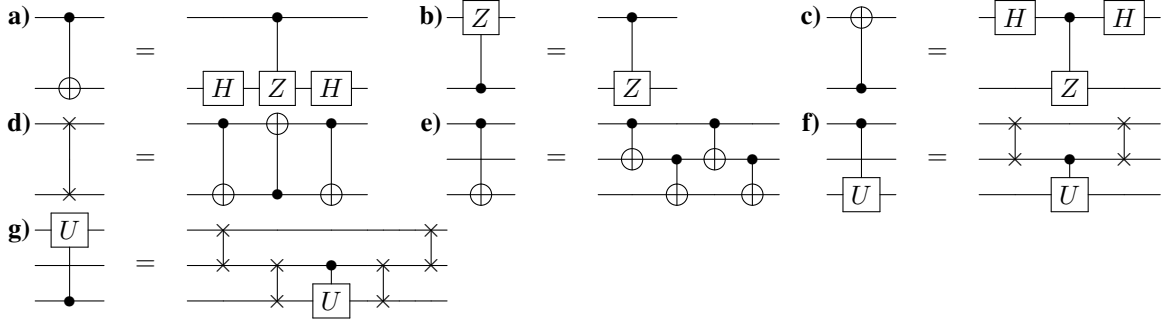


Figure 5. Implementation of some two-qubit gates available in the Instruction Set: a) CNOT-12; b) equivalence of CZ-12 and CZ-21; c) CNOT-21; d) SWAP; e) CNOT-13; f) generalized controlled gate with first qubit as control and third as target; g) generalized controlled gate with third qubit as control and first as target.

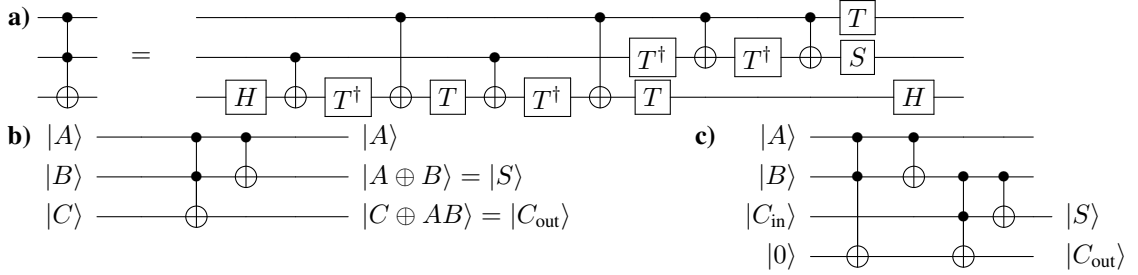


Figure 6. Implementation of three and four-qubit gates available in the Instruction Set : a) Toffoli (S , T and T^\dagger are nothing but $\sigma_z^{\frac{1}{2}}$, $\sigma_z^{\frac{1}{4}}$ and $\sigma_z^{-\frac{1}{4}}$ respectively); b) Peres, that behaves as Half-Adder for $|C\rangle = 0$; c) reversible Full-Adder.

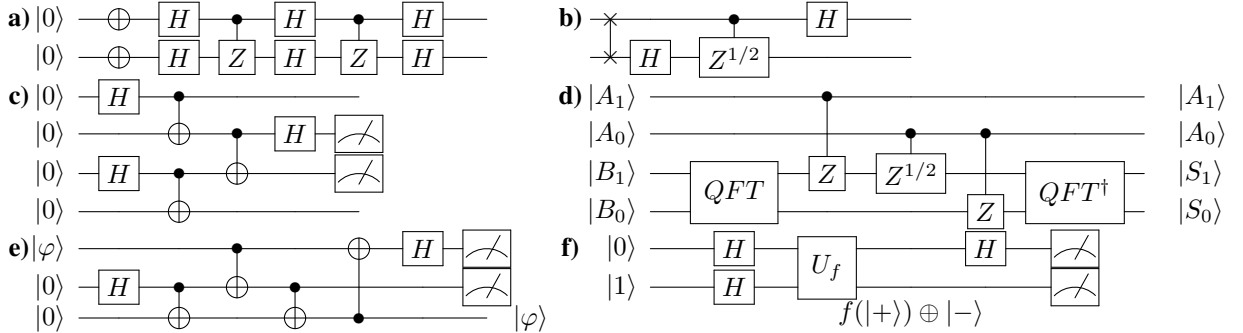


Figure 7. Some simulated algorithms: a) Grover's search; b) Quantum Fourier Transform; c) Entanglement Swapping; d) Quantum Addition; e) Quantum Teleportation; f) two-qubit Deutsch's algorithm.

right plots refer to molecules with \underline{J} and $\frac{1}{2}\underline{J}$ exchange factors respectively: as expected from the $B = 5$ T case, the reduction of \underline{J} terms by a factor two increases significantly the operating time intervals for the same magnetic field, or equivalently it is possible to obtain the same T_{UE} for lower static fields. Even though the $\frac{1}{2}\underline{J}$ molecules present a behavior much closer to the ideal one than the \underline{J} ones, they have not been synthesized, thus they are not involved in the timing analysis in Section VII.

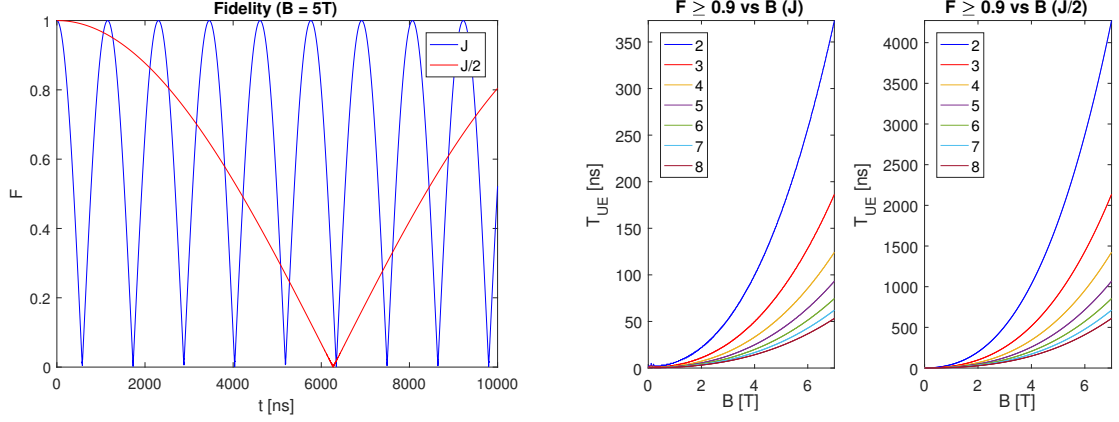
B. Decoherence

Similarly to the residual qubit-qubit interaction, a fidelity due to decoherence can be defined for non-interacting qubits subjected to Lindblad (Markovian) dynamics. In a worst case scenario, it is possible to define for a N -qubit molecule the following **decoherence error** equation [31]:

$$\epsilon_N = \frac{N}{2} \left(1 - e^{-\frac{t}{2T_M}} \right), \quad (18)$$

where T_M is the coherence time. It must be observed that decoherence affects not only the qubits but also the Co switch. According to the available informations [31], the decoherence of each qubit in molecule is considered independent from the applied magnetic field and equal to $T_M = 683$ ns for $T = 2.8$ K, while the switch decoherence depends on B . Considering the Supplementary Table 5 of [31], a dependence $T_{M_{sw}}(B)$ has been estimated though linear regression. It has been proved that for $B \geq 3$ T the Co switch decoherence occurs on a timescale longer than that of qubits, thus permitting to consider it negligible.

In order to establish the effect of decoherence on the reliability of results, the time duration τ_M for which the error ϵ_N is lower than 0.1 (thus $\mathcal{F} = \sqrt{1 - \epsilon_N} = 0.949 > 0.9$) has been computed, by exploiting Equation 18 with T_M fixed. It is possible to obtain $\tau_M = 144$ ns, $\tau_M = 94$ ns and $\tau_M = 70$ ns for the two, three and four-qubit molecules respectively.



(a) Fidelity time evolution of two two-qubit molecules with different inter-qubit exchange factors.

(b) Dependency of T_{UE} on the applied magnetic field for molecules with a number of qubits from two to eight (see the legend).

Figure 8. Analysis of the residual qubit-qubit interaction on the fidelity of the system. The values of the J tensor are those in [31].

VII. TIMING

It is possible to define a **time duration Δt for the implementation of quantum gates and algorithms** in which molecules (with the parameters in [31]) can be considered quasi-ideal. It is supposed that $\tau_M < T_{UE}$, *i.e.* the **shortest timescale is that associated to the qubit decoherence**; this condition can be reached by applying a sufficiently high static field ($B \sim 6$ T), with the drawback that the transition energies can belong to the infrared spectrum, especially for implementing the $C\phi$ gate ($150 \text{ GHz} \leq f \leq 560 \text{ GHz}$ approximately in a three-qubit device). The time interval for each gate/algorithm is computed by multiplying the longest sequence of gates from the system initialization to the final measurement by the pulse duration τ , with all gates executed in sequence and τ fixed; it is a worst case scenario, since there are some single rotations on different qubits than could be executed in parallel and circuits are not optimized in order to reduce the latency. The pulse duration τ , which differs between molecules with different number of qubits, is set to the highest value sufficient for ensuring that at least the 80% (so the majority) of the analyzed quantum instructions or algorithms satisfies the condition $\Delta t < \tau_M$. In particular, τ equals 5 ns, 1.7 ns and 0.47 ns for two, three and four-qubit nanomagnets respectively. It has been proved that the condition for a good approximation of the Controlled-phase gate is valid in all cases (see Appendix B).

In Table I, time durations of some simulated gates and algorithms are compared with the critical time duration. Quantum gates up to the reversible Full-Adder and the Deutsch's algorithm can be computed with negligible errors. For what concerns the two-qubit Grover's algorithm, timing constraints are satisfied only if single-qubit gates executable on different qubits at the same time - as the Hadamard or the $R_x(\pi)$ gates at the beginning of the algorithm (see the first quantum circuit in Figure 7) - are effectively executed simultaneously (*Grover P*). The purely sequential approach *Grover S* - where single-qubit gates on different qubits are not parallelized -

does not keep latency under threshold. In the molecule with three qubits, the controlled gates involving a couple of non-adjacent qubits, the Toffoli gate and the three-qubit Quantum Fourier Transform can be executed on a time interval lower than the critical one. The Grover's algorithm requires a so high number of gates that the timing requirements are not satisfied in both *S* and *P* cases. Since the four-qubit Grover's algorithm requires a number of iteration that is at least equal to that of the three-qubit one and the pulse duration τ is not reduced by a sufficient amount to ensure a significant latency reduction, the timing requirements are for sure not satisfied, so it has not been analyzed. The high number of SWAP gates required by the four-qubit Quantum Fourier Transform for applying the $C\phi$ gates between non-adjacent qubits does not permit to keep latency under the timing threshold.

VIII. SIMULATION

The simulation procedure of the current MATLAB infrastructure is exclusively functional, *i.e.* it only computes the state vectors after the application of quantum gates, without directly considering non-ideality phenomena and the quantum gates errors due to oscillations modulated by non-rectangular pulses. In other words, the simulator actually permits to define how a certain quantum algorithm can be executed on the analyzed $\text{Cr}_7\text{Ni-Co-Cr}_7\text{Ni}$ supramolecular complexes by exploiting their universal set of quantum gates. Each quantum circuit is decomposed into sequences of $R_x(\theta)$, $R_y(\theta)$ and $C\phi$ gates, then the comparison of the final state vectors - obtained by applying the unitary matrices of the developed model (see Appendices A and B) and those of ideal quantum gates - is done. However, it is already possible with the available simulator to regulate - according to the analysis of non-idealities previously discussed - the magnetostatic field B and the pulse duration τ , in order to estimate the qubits' transition frequencies. It can be concluded that the current simulation procedure is at a too preliminary stage for any type of comparison with other available simulation and real-hardware execution infrastructures, as those provided by IBM.

(a) Two-qubit ($\tau = 5$ ns, $\tau_M = 144$ ns)		(b) Three-qubit ($\tau = 1.7$ ns, $\tau_M = 94$ ns)		(c) Four-qubit ($\tau = 0.47$ ns, $\tau_M = 70$ ns)	
Gate	Δt [ns]	Gate	Δt [ns]	Gate	Δt [ns]
Hadamard	10	Toffoli	81.6	Toffoli-124	39.48
$C\phi$	10	Half-Adder	91.6	Full-Adder	67.68
CNOT-12	30	QFT	81.6	Deutsch	36.66
SWAP	90	Teleportation	88.4	Ent. Swapping	11.28
QFT	120	Deutsch	64.6	Addition	42.30
Grover S	200	Grover S	375.7	QFT	144.80
Grover P	110	Grover P	324.7		

Table I
LATENCY OF SOME SIMULATED OPERATIONS AND ALGORITHMS.

However, for sake of completeness, a comparison between Quantum Teleportation (see Figure 7) on a simulated three-qubit molecular nanomagnet and on the superconducting real quantum computer IBM Q 5 Tenerife (ibmqx4) - programmed through the [IBM Q Experience website](#) - is reported: the two technologies can be actually compared in terms of implementation of the quantum circuit and equivalences of the results. Non-idealities are assumed to negligibly contribute in both cases; for this reason, the operating point for the manipulation of the spin qubits of the molecular nanomagnet is set to $B = 7$ T and $\tau = 1.7$ ns, coherently with the analysis in Sections VI and VII, while the averaging of the results of multiple experiments - performed on ibmqx4 with the same last calibration and number of shots fixed to 1024 - has been done. Assuming that in both cases the qubits are all initialized

error $\Delta|c_{ijk}|^2$, *i.e.* the difference between the probabilities computed by the molecular simulator and by the ideal unitary matrices, while the rightmost report the mean value and the standard deviation of each measured probability on the real quantum computer P_{ibmqx4} . It is remarked that the effective errors for the molecule would be much larger if non-ideality models were directly inserted in the simulation. For what

	$c_{ijk\text{mol}}$	$\Delta c_{ijk} ^2$ [$\times 10^{-3}$]	$\mu (P_{\text{ibmqx4}})$	$\sigma (P_{\text{ibmqx4}})$ [$\times 10^{-3}$]
[000]	0.2891 + 0.0010 i	-0.24	0.120	5
[001]	0.2893 + 0.0012 i	-0.35	0.106	14
[010]	0.2881 + 0.0010 i	0.35	0.062	3
[011]	0.2883 + 0.0012 i	0.24	0.062	5
[100]	-0.0016 + 0.4079 i	0.24	0.217	16
[101]	-0.0008 + 0.4085 i	-0.24	0.148	10
[110]	-0.0023 + 0.4079 i	0.24	0.147	13
[111]	-0.0014 + 0.4085 i	-0.24	0.137	12

Table II

RESULTS OF QUANTUM TELEPORTATION SIMULATION.

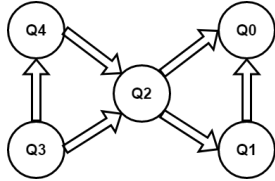


Figure 9. Connectivity of IBM Q 5 Tenerife (ibmqx4) quantum computer.

to $|0\rangle$, Teleportation procedure is executed after applying to the upper bit the sequence $R_z(\pi)R_x(1.9106)$, such that the the information to be moved from one qubit to another is $|\varphi\rangle = \frac{|0\rangle + i\sqrt{2}|1\rangle}{\sqrt{3}}$. Differently from what introduced in the previous, an optimized circuit of the protocol is reported in both cases (Figure 10). It is precised that qubits are bottom-up ordered, *i.e.* the most significant qubit corresponds to the lowest one in the quantum circuit.

It can be clearly observed that the molecular implementation requires an higher number of quantum gates than the superconducting one (eighteen instead of eleven) mainly for two reasons: on the one hand the CNOT gate is not native, *i.e.* it must be constructed from Hadamard and CZ gates, on the other the connectivity of qubits is linear (see Figure 3(b)), thus requiring SWAP gates in order to close non-adjacent qubits, while the triangular connectivity of qubits Q0, Q1 and Q2 on ibmqx4 (see Figure 9) permits to avoid SWAP operations. The results are available in Table II: the two leftmost columns report the probability amplitudes $c_{ijk\text{mol}}$ for each basis state computed by MATLAB functions and the probability absolute

concerns the molecular nanomagnet, measurement operation has not been simulated, but it is possible to conclude - considering the periodicity of $c_{ijk\text{mol}}$ coefficients - that the probabilities of the basis states with most significant qubit equal to $|0\rangle$ are roughly $\frac{1}{3} \cdot \frac{1}{4} \simeq 0.083$, while for those with least significant qubit equal to $|1\rangle$ it is $\frac{2}{3} \cdot \frac{1}{4} \simeq 0.167$, as theoretically expected. The absolute errors - due to the calculations of the approximated Controlled-phase gate - are all lower than 1×10^{-3} , while relative errors, they are less than 1%, so they can be reasonably treated as negligible. The probabilities of measuring on the superconducting quantum computer $q[2] = 0$ and $q[2] = 1$, given by the sum of the probabilities of the basis states with the same value of $q[2]$, are close to the expected ones; in fact, they are equal to 0.35 and 0.65 respectively, *i.e.* they deviate from the expected results in ideal conditions by +5% and -2% respectively, thus proving the functional equivalences of the quantum circuits in Figure 10.

IX. CONCLUSIONS

A mathematical model and a potential quantum computer architecture with molecular nanomagnets are proposed in this work, taking into account the non-idealities of the target technology. The realized MATLAB infrastructure has been developed in order to be easily extendable to other molecular technologies for quantum computing. The results obtained

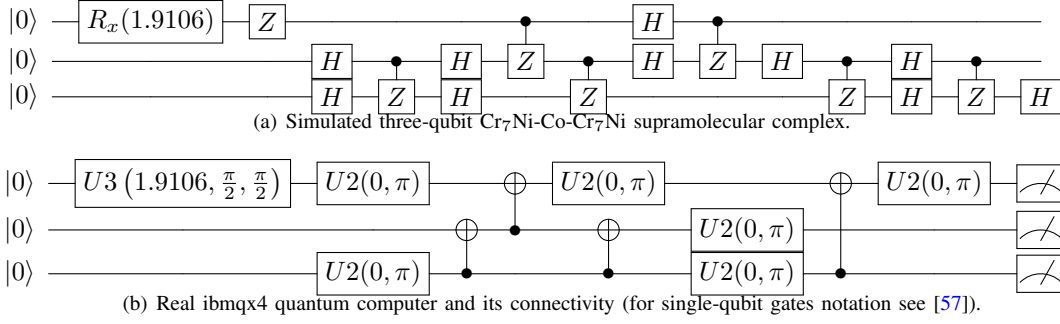


Figure 10. Optimized quantum circuits for teleportation.

can be considered optimistic for the feasibility of a quantum computer based on Cr_7Ni supramolecular complexes, since the DiVincenzo criteria for quantum computers could be totally satisfied in the next decades.

In order to obtain a system reliable on larger timescales, quantum information must be protected from errors due to decoherence and other quantum noise (faulty quantum gates, quantum preparation and measurements); for these reasons, strategies for avoiding possible errors should be analyzed as Quantum Error Correction (QEC) and quantum gates optimization, from both the physical implementation - *e.g.* the so-called virtual-Z gates [58] - and circuit compilation points of view.

For what concerns simulation, a sophisticated simulator for molecular quantum computing must be developed, where the results of a certain algorithm are evaluated in "ideal" and "real" conditions, *i.e.* under the effect of non-idealities. Moreover, the simulator should permit on the one hand to regulate physical parameters as the magnetostatic field, the frequencies of the external signals to be provided to the spin qubits and the shapes of the modulating signals, whose choice influences the final results, on the other it could be employed in a "hardware-abstraction" mode, where users can design their quantum circuits with a technology-independent language as the intermediate-level OpenQASM [57], without the necessity to learn the internal routines of the simulator.

The computer architecture perspectives and goals require the parallel support of chemical engineering, through the synthesis of molecules with more qubits connected in a structure more complex than linear and characterized by longer timescales of non-idealities. For what concerns the qubits connectivity, it has been ascertained that the creation of qubit arrays from single-qubit molecular building units do not necessarily ensure the preservation of single-qubit coherence and relaxation timescales, because the reciprocal inter-qubit distances and the molecular crystal lattice phonon structure may be modified [59]. Three-dimensional Metal-Organic Frameworks (MOFs) have been already analyzed for the fabrication of vanadyl [59] or Cu^{2+} [60] qubit arrays, linked through tetracarboxylphenyl-porphyrinate ligands in both cases. Lanthanide ion spin qubits have been recently analyzed when combined with peptides: this biomolecular approach seems to facilitate the preparation of new structures, with customizable properties (*e.g.* coherence timescales) and spatial organization [61].

Decoherence timescales of $15\mu\text{s}$ have been already reached for synthesized Cr_7Ni rings [46] and their insertion in supramolecular complexes would be an essential step towards a reliable and scalable quantum computing architecture.

APPENDIX A SPIN- $\frac{1}{2}$ MANIPULATION

Given a static magnetic field $\mathbf{B}_0 = B_0\mathbf{z}$ and an oscillating magnetic field $\mathbf{B}_1 = 2B_1 \cos(\omega t - \phi)\mathbf{x}$ applied on a spin- $\frac{1}{2}$ quantum system with gyromagnetic ratio γ , the spin precesses about the z -axis and the xy -plane at angular frequencies $\omega_0 = \gamma B_0$ and $\omega_1 = \gamma B_1$ respectively. However, the precession about the xy -plane at frequency ω_1 is successful if and only if the oscillation frequency ω is equal to ω_0 , which is the transition frequency required for changing the spin orientation. The spin unitary evolution on a time interval τ in a frame rotating with frequency ω_0 around the z -axis can be written as:

$$U = \begin{bmatrix} \cos\left(\frac{\Omega\tau}{2}\right) - i\frac{\delta}{\Omega}\sin\left(\frac{\Omega\tau}{2}\right) & \frac{\omega_1}{\Omega}\sin\left(\frac{\Omega\tau}{2}\right)e^{-i(\frac{\pi}{2}+\phi)} \\ \frac{\omega_1}{\Omega}\sin\left(\frac{\Omega\tau}{2}\right)e^{-i(\frac{\pi}{2}-\phi)} & \cos\left(\frac{\Omega\tau}{2}\right) + i\frac{\delta}{\Omega}\sin\left(\frac{\Omega\tau}{2}\right) \end{bmatrix} \quad (19)$$

where $\Omega = \sqrt{\omega_1^2 + \delta^2}$ is the **Rabi frequency** and $\delta = \omega - \omega_0$ is the **detuning**. The magnitude square of the terms on the anti-diagonal is equal to the transition/rotation probability

$$P_{|0\rangle \leftrightarrow |1\rangle} = \left| \frac{\omega_1}{\Omega} \sin\left(\frac{\Omega\tau}{2}\right) \right|^2. \quad (20)$$

When the carrier signal is resonant with the transition - *i.e.* $\delta = 0$ and $\Omega = \omega_1$ - the unitary evolution matrix can be simplified

$$\tilde{U} = \begin{bmatrix} \cos\left(\frac{\omega_1\tau}{2}\right) & \sin\left(\frac{\omega_1\tau}{2}\right)e^{-i(\frac{\pi}{2}+\phi)} \\ \sin\left(\frac{\omega_1\tau}{2}\right)e^{-i(\frac{\pi}{2}-\phi)} & \cos\left(\frac{\omega_1\tau}{2}\right) \end{bmatrix}. \quad (21)$$

It is possible to observe that $\omega_1\tau = \theta$, *i.e.* these parameters are related to the amount of spin rotation θ around an axis on xy -plane depending on the phase ϕ ; $R_x(\theta)$ and $R_y(\theta)$ gate are obtained for $\phi = 0$ in the first case and $\phi = \frac{\pi}{2}$ respectively.

APPENDIX B APPROXIMATION OF THE CONTROLLED-PHASE GATE

The rotating frame does not permit to estimate correctly the unitary evolution of a spin when $|\delta| \rightarrow \infty$. This can be critical for describing the spin switch evolution when the external

excitation is not resonant with its transition frequency, *i.e.* when the adjacent qubits are equal to $|00\rangle$, $|01\rangle$ or $|10\rangle$. An approximated model has been exploited for the $C\phi$ gate, in order to reach a compromise between its effective unitary evolution and the simple equations of the spin- $\frac{1}{2}$ evolution in the rotating frame. Each pulse rotating the spin switch is described by a diagonal matrix $M = \text{diag}([e^{iP_{00}\phi}, e^{iP_{01}\phi}, e^{iP_{10}\phi}, e^{iP_{11}\phi}])$, where P_{ij} is the transition probability $|ij\rangle (|S_{zsw}\rangle = |-\frac{1}{2}\rangle) \Leftrightarrow |ij\rangle (|S_{zsw}\rangle = |+\frac{1}{2}\rangle)$. The total $C\phi$ gate would be obtained by applying two pulses, with phases $-\phi_1$ and ϕ_2 respectively; since P_{ij} does not change in the pulse sequence, the gate can be described in terms of matrix product as

$$M_2 M_1 = \begin{bmatrix} e^{iP_{00}\Delta\phi} & 0 & 0 & 0 \\ 0 & e^{iP_{01}\Delta\phi} & 0 & 0 \\ 0 & 0 & e^{iP_{10}\Delta\phi} & 0 \\ 0 & 0 & 0 & e^{iP_{11}\Delta\phi} \end{bmatrix}, \quad (22)$$

with $\Delta\phi = \phi_2 - \phi_1$. For sake of simplicity, ϕ_2 and ϕ_1 can be set to ϕ and 0 respectively. Since the transition frequencies $|ij\rangle (|S_{zsw}\rangle = |-\frac{1}{2}\rangle) \Leftrightarrow |ij\rangle (|S_{zsw}\rangle = |+\frac{1}{2}\rangle)$ are sufficiently different for ensuring, for $\omega_1\tau = \pi$, a transition probability equal to 1 for $|11\rangle$ and $P_{ij}\phi \ll 1$ for $|ij\rangle \neq |11\rangle$ on time scales of some nanosecond, the product of the matrices would be approximately a $C\phi$.

For the definition of the approximated model, it is supposed that $P\phi \leq \frac{1}{10}$ is sufficient for a negligible phase of the complex exponential. Since $\phi \leq \pi$ in all the cases of interest, the transition probability must be $P \leq \frac{1}{10\pi} = 0.032$, that can be treated as a negligible value even in the canonical model. According to Equation 20, it is possible to derive

$$\max\{P\} = \left| \frac{\omega_1}{\Omega} \right|^2 = \frac{1}{1 + \left(\frac{\delta}{\omega_1} \right)^2} \leq \frac{1}{10\pi}, \quad (23)$$

and consequently $\left(\frac{\delta}{\omega_1} \right)^2 \geq 10\pi - 1$. Neglecting the -1 term with the respect to 10π , since each spin pulse provides a π rotation and consequently $\omega_1 = \frac{\pi}{\tau}$, the condition ensuring a good approximation is

$$\frac{\delta\tau}{\pi} \geq \sqrt{10\pi} \Rightarrow \delta_f\tau \geq \sqrt{\frac{5\pi}{2}} \approx 2.8, \quad (24)$$

where $\delta_f = \frac{\delta}{2\pi}$.

REFERENCES

- [1] "International Technology Roadmap of Semiconductors 2.0. Beyond CMOS." 2015, <http://public.itrs.net>.
- [2] M. A. Nielsen and I. L. Chuang, *Quantum Computation and Quantum Information: 10th Anniversary Edition*, 10th ed. New York, NY, USA: Cambridge University Press, 2011.
- [3] P. W. Shor, "Polynomial-time algorithms for prime factorization and discrete logarithms on a quantum computer," *SIAM review*, vol. 41, no. 2, pp. 303–332, 1999.
- [4] J. Clarke and F. K. Wilhelm, "Superconducting quantum bits," *Nature*, vol. 453, no. 7198, p. 1031, 2008.
- [5] J. M. Chow, *Quantum information processing with superconducting qubits*. Yale University, 2010.
- [6] M. H. Devoret and R. J. Schoelkopf, "Superconducting circuits for quantum information: an outlook," *Science*, vol. 339, no. 6124, pp. 1169–1174, 2013.
- [7] P. Krantz, M. Kjaergaard, F. Yan, T. P. Orlando, S. Gustavsson, and W. D. Oliver, "A quantum engineer's guide to superconducting qubits," *Applied Physics Reviews*, vol. 6, no. 2, p. 021318, 2019. [Online]. Available: <https://doi.org/10.1063/1.5089550>
- [8] C. D. Bruzewicz, J. Chiaverini, R. McConnell, and J. M. Sage, "Trapped-ion quantum computing: Progress and challenges," *Applied Physics Reviews*, vol. 6, no. 2, p. 021314, 2019. [Online]. Available: <https://doi.org/10.1063/1.5088164>
- [9] P. Kok, W. J. Munro, K. Nemoto, T. C. Ralph, J. P. Dowling, and G. J. Milburn, "Linear optical quantum computing with photonic qubits," *Reviews of Modern Physics*, vol. 79, no. 1, p. 135, 2007.
- [10] J. L. O'Brien, "Optical quantum computing," *Science*, vol. 318, no. 5856, pp. 1567–1570, 2007.
- [11] C. Nayak, S. H. Simon, A. Stern, M. Freedman, and S. Das Sarma, "Non-abelian anyons and topological quantum computation," *Rev. Mod. Phys.*, vol. 80, pp. 1083–1159, Sep 2008. [Online]. Available: <https://link.aps.org/doi/10.1103/RevModPhys.80.1083>
- [12] J. D. Sau, R. M. Lutchyn, S. Tewari, and S. Das Sarma, "Generic new platform for topological quantum computation using semiconductor heterostructures," *Phys. Rev. Lett.*, vol. 104, p. 040502, Jan 2010. [Online]. Available: <https://link.aps.org/doi/10.1103/PhysRevLett.104.040502>
- [13] D. Loss and D. P. DiVincenzo, "Quantum computation with quantum dots," *Physical Review A*, vol. 57, no. 1, p. 120, 1998.
- [14] B. E. Kane, "A silicon-based nuclear spin quantum computer," *nature*, vol. 393, no. 6681, p. 133, 1998.
- [15] J. J. Morton, D. R. McCamey, M. A. Eriksson, and S. A. Lyon, "Embracing the quantum limit in silicon computing," *Nature*, vol. 479, no. 7373, p. 345, 2011.
- [16] R. Maurand, X. Jehl, D. Kotekar-Patil, A. Corna, H. Bohuslavskiy, R. Laviéville, L. Hutin, S. Barraud, M. Vinet, M. Sanquer *et al.*, "A CMOS silicon spin qubit," *Nature communications*, vol. 7, p. 13575, 2016.
- [17] D. Cory, A. Fahmy, and T. Havel, "Ensemble quantum computing by NMR spectroscopy," *Proceedings of the National Academy of Sciences of the United States of America*, vol. 94, no. 5, pp. 1634–1639, 1997.
- [18] L. M. Vandersypen and I. L. Chuang, "NMR techniques for quantum control and computation," *Reviews of modern physics*, vol. 76, no. 4, p. 1037, 2005.
- [19] I. Oliveira, R. Sarthour, T. Bonagamba, E. deAzevedo, and J. Freitas, *NMR Quantum Information Processing*. Elsevier, 2007.
- [20] M. Nakahara and T. Ohmi, *Quantum computing: from linear algebra to physical realizations*. CRC press, 2008.
- [21] T. Xin, B.-X. Wang, K.-R. Li, X.-Y. Kong, S.-J. Wei, T. Wang, D. Ruan, and G.-L. Long, "Nuclear magnetic resonance for quantum computing: Techniques and recent achievements," *Chinese Physics B*, vol. 27, no. 2, p. 020308, feb 2018. [Online]. Available: <https://doi.org/10.1088%2F1674-1056%2F27%2F2%2F020308>
- [22] S. Sproules, "Molecules as electron spin qubits," in *Electron Paramagnetic Resonance: Volume 25*. The Royal Society of Chemistry, 2017, vol. 25, pp. 61–97. [Online]. Available: <http://dx.doi.org/10.1039/9781782629436-00061>
- [23] J. Jones, M. Mosca, and R. Hansen, "Implementation of a quantum search algorithm on a quantum computer," *Nature*, vol. 393, no. 6683, pp. 344–346, 1998.
- [24] L. M. Vandersypen, M. Steffen, G. Breyta, C. S. Yannoni, M. H. Sherwood, and I. L. Chuang, "Experimental realization of shor's quantum factoring algorithm using nuclear magnetic resonance," *Nature*, vol. 414, no. 6866, p. 883, 2001.
- [25] F. Vind, A. Foerster, I. Oliveira, R. Sarthour, D. Soares-Pinto, A. Souza, and I. Roditi, "Experimental realization of the yang-baxter equation via nmr interferometry," *Scientific Reports*, vol. 6, 2016.
- [26] X. Peng, J. Zhang, J. Du, and D. Suter, "Quantitative complementarity between local and nonlocal character of quantum states in a three-qubit system," *Physical Review A - Atomic, Molecular, and Optical Physics*, vol. 77, no. 5, 2008.
- [27] J. Pan, Y. Cao, X. Yao, Z. Li, C. Ju, H. Chen, X. Peng, S. Kais, and J. Du, "Experimental realization of quantum algorithm for solving linear systems of equations," *Phys. Rev. A*, vol. 89, p. 022313, Feb 2014. [Online]. Available: <https://link.aps.org/doi/10.1103/PhysRevA.89.022313>
- [28] W.-L. Chang and A. V. Vasilakos, *Molecular Computing: Towards a Novel Computing Architecture for Complex Problem Solving*. Springer, 2014, vol. 4.
- [29] W.-L. Chang, T.-T. Ren, and M. Feng, "Quantum algorithms and mathematical formulations of biomolecular solutions of the vertex cover

- problem in the finite-dimensional hilbert space,” *IEEE transactions on nanobioscience*, vol. 14, no. 1, pp. 121–128, 2015.
- [30] W.-L. Chang, Q. Yu, Z. Li, J. Chen, X. Peng, and M. Feng, “Quantum speedup in solving the maximal-clique problem,” *Phys. Rev. A*, vol. 97, p. 032344, Mar 2018. [Online]. Available: <https://link.aps.org/doi/10.1103/PhysRevA.97.032344>
 - [31] J. Ferrando-Soria, E. M. Pineda, A. Chiesa, A. Fernandez, S. A. Magee, S. Carretta, P. Santini, I. J. Vitorica-Yrezabal, F. Tuna, G. A. Timco, E. J. McInnes, and R. E. Winpenny, “A modular design of molecular qubits to implement universal quantum gates,” *Nature communications*, vol. 7, p. 11377, 2016.
 - [32] L. Escalera-Moreno, J. J. Baldoví, A. Gaita-Ariño, and E. Coronado, “Spin states, vibrations and spin relaxation in molecular nanomagnets and spin qubits: a critical perspective,” *Chem. Sci.*, vol. 9, pp. 3265–3275, 2018. [Online]. Available: <http://dx.doi.org/10.1039/C7SC05464E>
 - [33] J. Tejada, E. Chudnovsky, E. Del Barco, J. Hernandez, and T. Spiller, “Magnetic qubits as hardware for quantum computers,” *Nanotechnology*, vol. 12, no. 2, p. 181, 2001.
 - [34] M. N. Leuenberger and D. Loss, “Quantum computing in molecular magnets,” *Nature*, vol. 410, no. 6830, p. 789, 2001.
 - [35] M. J. Graham, J. M. Zadrozny, M. S. Fataftah, and D. E. Freedman, “Forging solid-state qubit design principles in a molecular furnace,” *Chemistry of Materials*, vol. 29, no. 5, pp. 1885–1897, 2017. [Online]. Available: <https://doi.org/10.1021/acs.chemmater.6b05433>
 - [36] A. Gaita-Ariño, F. Luis, S. Hill, and E. Coronado, “Molecular spins for quantum computation,” *Nature chemistry*, vol. 11, no. 4, p. 301, 2019.
 - [37] M. Atzori and R. Sessoli, “The second quantum revolution: Role and challenges of molecular chemistry,” *Journal of the American Chemical Society*, vol. 0, no. 0, p. null, 0, pMID: 31287678. [Online]. Available: <https://doi.org/10.1021/jacs.9b00984>
 - [38] J. J. Baldoví, S. Cardona-Serra, J. M. Clemente-Juan, E. Coronado, A. Gaita-Ariño, and H. Prima-García, “Coherent manipulation of spin qubits based on polyoxometalates: the case of the single ion magnet [GdW₃₀P₅O₁₁₀]^{14−},” *Chemical Communications*, vol. 49, no. 79, pp. 8922–8924, 2013.
 - [39] M. Jenkins, Y. Duan, B. Diosdado, J. García-Ripoll, A. Gaita-Ariño, C. Giménez-Saiz, P. Alonso, E. Coronado, and F. Luis, “Coherent manipulation of three-qubit states in a molecular single-ion magnet,” *Physical Review B*, vol. 95, no. 6, p. 064423, 2017.
 - [40] C. Godfrin, R. Ballou, E. Bonet, M. Ruben, S. Klyatskaya, W. Wernsdorfer, and F. Balestro, “Generalized ramsey interferometry explored with a single nuclear spin qubit,” *npj Quantum Information*, vol. 4, no. 1, p. 53, 2018.
 - [41] C. Godfrin, A. Ferhat, R. Ballou, S. Klyatskaya, M. Ruben, W. Wernsdorfer, and F. Balestro, “Operating quantum states in single magnetic molecules: Implementation of grover’s quantum algorithm,” *Physical review letters*, vol. 119, no. 18, p. 187702, 2017.
 - [42] M. Jenkins, D. Zueco, O. Roubeau, G. Aromí, J. Majer, and F. Luis, “A scalable architecture for quantum computation with molecular nanomagnets,” *Dalton Transactions*, vol. 45, no. 42, pp. 16 682–16 693, 2016.
 - [43] J. M. Zadrozny, J. Niklas, O. G. Poluektov, and D. E. Freedman, “Millisecond coherence time in a tunable molecular electronic spin qubit,” *ACS Central Science*, vol. 1, no. 9, pp. 488–492, 2015, pMID: 27163013. [Online]. Available: <https://doi.org/10.1021/acscentsci.5b00338>
 - [44] F. Luis, A. Repollés, M. J. Martínez-Pérez, D. Aguilá, O. Roubeau, D. Zueco, P. J. Alonso, M. Evangelisti, A. Camón, J. Sesé *et al.*, “Molecular prototypes for spin-based cnot and swap quantum gates,” *Physical review letters*, vol. 107, no. 11, p. 117203, 2011.
 - [45] A. M. Repollés Rabinad, *Quantum computing with molecular magnets*. Prensas de la Universidad de Zaragoza, 2016, vol. 131.
 - [46] C. J. Wedge, G. Timco, E. Spielberg, R. George, F. Tuna, S. Rigby, E. McInnes, R. Winpenny, S. Blundell, and A. Ardavan, “Chemical engineering of molecular qubits,” *Physical review letters*, vol. 108, no. 10, p. 107204, 2012.
 - [47] A. Chiesa, P. Santini, and S. Carretta, “Supramolecular complexes for quantum simulation,” *Magnetochemistry*, vol. 2, no. 4, p. 37, 2016.
 - [48] R. P. Feynman, “Simulating physics with computers,” *International journal of theoretical physics*, vol. 21, no. 6, pp. 467–488, 1982.
 - [49] S. Lloyd, “Universal quantum simulators,” *Science*, pp. 1073–1078, 1996.
 - [50] L. Sanchez-Palencia, “Quantum simulation: From basic principles to applications: Foreword,” *Comptes Rendus Physique*, vol. 19, no. 6, pp. 357 – 364, 2018, quantum simulation / Simulation quantique. [Online]. Available: <http://www.sciencedirect.com/science/article/pii/S1631070518301245>
 - [51] D. P. DiVincenzo, “The physical implementation of quantum computation,” *Fortschritte der Physik*, vol. 48, no. 9-11, pp. 771–783, 2000. [Online]. Available: <https://onlinelibrary.wiley.com/doi/abs/10.1002/1521-3978%28200009%2948%3A9%11%3C771%3A%3AAID-PROP771%3E3.0.CO%3B2-E>
 - [52] D. Deutsch and R. Jozsa, “Rapid solution of problems by quantum computation,” *Proc. R. Soc. Lond. A*, vol. 439, no. 1907, pp. 553–558, 1992.
 - [53] L. K. Grover, “A fast quantum mechanical algorithm for database search,” in *Proceedings of the Twenty-eighth Annual ACM Symposium on Theory of Computing*, ser. STOC ’96. New York, NY, USA: ACM, 1996, pp. 212–219. [Online]. Available: <http://doi.acm.org/10.1145/237814.237866>
 - [54] —, “Quantum mechanics helps in searching for a needle in a haystack,” *Physical review letters*, vol. 79, no. 2, p. 325, 1997.
 - [55] B. Coecke, *The Logic of Entanglement*. Cham: Springer International Publishing, 2014, pp. 250–267. [Online]. Available: https://doi.org/10.1007/978-3-319-06880-0_13
 - [56] T. G. Draper, “Addition on a quantum computer,” *arXiv preprint quant-ph/0008033*, 2000.
 - [57] A. W. Cross, L. S. Bishop, J. A. Smolin, and J. M. Gambetta, “Open quantum assembly language,” *arXiv preprint arXiv:1707.03429*, 2017.
 - [58] D. C. McKay, C. J. Wood, S. Sheldon, J. M. Chow, and J. M. Gambetta, “Efficient z gates for quantum computing,” *Phys. Rev. A*, vol. 96, p. 022330, Aug 2017. [Online]. Available: <https://link.aps.org/doi/10.1103/PhysRevA.96.022330>
 - [59] T. Yamabayashi, M. Atzori, L. Tesi, G. Cosquer, F. Santanni, M.-E. Boulon, E. Morra, S. Benci, R. Torre, M. Chiesa, L. Sorace, R. Sessoli, and M. Yamashita, “Scaling up electronic spin qubits into a three-dimensional metal–organic framework,” *Journal of the American Chemical Society*, vol. 140, no. 38, pp. 12 090–12 101, 2018, pMID: 30145887. [Online]. Available: <https://doi.org/10.1021/jacs.8b06733>
 - [60] C.-J. Yu, M. D. Krzyaniak, M. S. Fataftah, M. R. Wasielewski, and D. E. Freedman, “A concentrated array of copper porphyrin candidate qubits,” *Chem. Sci.*, vol. 10, pp. 1702–1708, 2019. [Online]. Available: <http://dx.doi.org/10.1039/C8SC04435J>
 - [61] L. E. Rosaleny, S. Cardona-Serra, L. Escalera-Moreno, J. J. Baldoví, V. Golebiewska, K. Wlazlo, P. Casino, H. Prima-García, A. Gaita-Ariño, and E. Coronado, “Peptides as versatile platforms for quantum computing,” *The Journal of Physical Chemistry Letters*, vol. 9, no. 16, pp. 4522–4526, 2018, pMID: 30044106. [Online]. Available: <https://doi.org/10.1021/acs.jpclett.8b01813>

Giovanni Amedeo Cirillo received the B.Sc. and M.Sc. degrees in Electronic Engineering – in 2016 and 2018 respectively – from Politecnico di Torino, where is pursuing the Ph.D. degree in Electrical, Electronics and Communications Engineering. His research activities mainly focus on technological modelling and architectural design for Quantum Computing.

Giovanna Turvani received the M.Sc. degree with honors (*Magna Cum Laude*) in Electronic Engineering in 2012 and the Ph.D. degree from the Politecnico di Torino. She was Postdoctoral Research Associate at the Technical University of Munich in 2016. She is currently Postdoctoral Research Associate at Politecnico di Torino. Her interests include CAD Tools development for non-CMOS nanocomputing, architectural design for field-coupled nanocomputing and high-level device modeling. She is currently involved in a national project on microwave imaging technology for brain stroke monitoring.

Mariagrazia Graziano received the Dr.Eng. degree and the Ph.D in Electronics Engineering from the Politecnico di Torino, Italy, in 1997 and 2001, respectively. Since 2002 she is Assistant Professor at the Politecnico di Torino. Since 2008 she is adjunct Faculty at the University of Illinois at Chicago and since 2014 she is a Marie-Curie fellow at the London Centre for Nanoelectronics. She works on “beyond CMOS” devices, circuits and architectures.